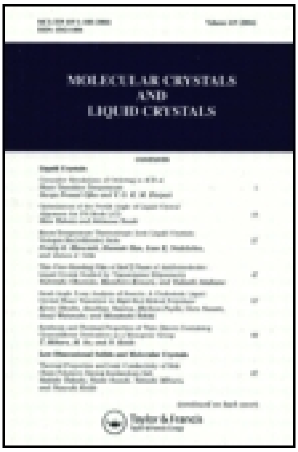

Molecular Crystals and Liquid Crystals
Publication details, including instructions for authors and subscription information:
http://www.tandfonline.com/loi/gmcl20

# Dielectric Spectroscopy of Bent-Core Thioesters' B Phases

J. Chruściel [a] , M. Wierzejska-Adamowicz [b] , D. M. Ossowska-Chruściel [a] , M. Marzec [b] , A. Wawrzyniak [b] , R. Douali [c] , Ch. Legrand [c] & S. Wróbel [b]

[a] Institute of Chemistry, Siedlce University of Natural Sciences and Humanities, Siedlce, Poland

[b] Jagiellonian University, Institute of Physics, Reymonta, Kraków, Poland

[c] Université du Littoral Côte d'Opale, LEMCEL, Calais, France

Version of record first published: 30 Jun 2011

To cite this article: J. Chruściel, M. Wierzejska-Adamowicz, D. M. Ossowska-Chruściel, M. Marzec, A. Wawrzyniak, R. Douali, Ch. Legrand & S. Wróbel (2011): Dielectric Spectroscopy of Bent-Core Thioesters' B Phases, Molecular Crystals and Liquid Crystals, 541:1, 252/[490]-261/[499]

To link to this article: http://dx.doi.org/10.1080/15421406.2011.569249

*Mol. Cryst. Liq. Cryst.*, Vol. 541: pp. 252/[490]–261/[499], 2011

ISSN: 1542-1406 print/1563-5287 online
DOI: 10.1080/15421406.2011.569249

Taylor & Francis
Taylor & Francis Group

# Dielectric Spectroscopy of Bent-Core Thioesters' B Phases

J. CHRUŚCIEL,[1] M. WIERZEJSKA-ADAMOWICZ,[2]
D. M. OSSOWSKA-CHRUŚCIEL,[1] M. MARZEC,[2]
A. WAWRZYNIAK,[2] R. DOUALI,[3] CH. LEGRAND,[3]
AND S. WRÓBEL[2]

[1]Institute of Chemistry, Siedlce University of Natural Sciences and Humanities, Siedlce, Poland
[2]Jagiellonian University, Institute of Physics, Reymonta, Kraków, Poland
[3]Université du Littoral Côte d'Opale, LEMCEL, Calais, France

*Banana-shaped homologoues 1,3-phenylene bis{4-[(4-alkoxybenzoyl) sulfanyl]benzoate}, in short nOSOR, where n denotes the number of carbon atoms in the end chains, have been studied using dielectric and electrooptic methods. 9OSOR shows a ferroelectric $B_1$ phase, whereas 12OSOR, 14OSOR exhibit antiferroelectric $B_2$ phase. Dielectric spectra have been measured for two alignments of $B_2$ phase. In the low frequency range a broad collective relaxation process is observed under bias field. This process is connected with fluctuations of ferroelectric domains. The high frequency relaxation originates from molecular reorientation around the long axis.*

**Keywords** Banana-shaped mesogenes; collective modes; dielectric relaxation; molecular processes

## 1. Introduction

Liquid crystals composed of banana-shaped molecules belong to a new interesting class of liquid crystals [1,2]. Smectic B phases of banana-shaped systems differ from typical ferroelectric and antiferroelectric smectic phases studied so far. These new materials attract our attention because of unexpected electro-optic properties, i.e., fast switching from planar to homeotropic state for the secondary optical axis [3,4].

The $B_2$ phase can have four possible structures: synclinic – antiferroelectric, antyclinic – antiferroelectric, synclinic – ferroelectric and antyclinic – ferroelectric [5,6]. Two antiferroelectric states usually appear as ground state and two ferroelectric states can be obtained by applying an external electric field [6,7]. Different types of $B_2$ phases can be distinguished by using complementary methods: texture observation, electro-optic response and X-ray diffraction.

---

Address correspondence to S. Wróbel, Jagiellonian University, Institute of Physics, Reymonta 4, Pl-30-059 Kraków, Poland. Tel.: +48(12)6635684; E-mail: stanislaw.wrobel@uj.edu.pl

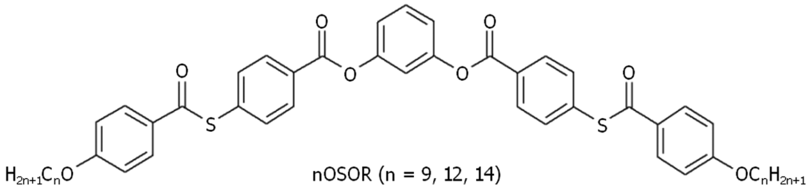

**Figure 1.** Molecular structure of bent-core mesogenes studied and their phase diagrams obtained during cooling.

In this work dielectric and electrooptic methods were used to investigate B phases of three symmetric bent-core thioestr mesogenes nOSOR ($n = 9$, 12, 14) (Fig. 1). 9OSOR shows ferroelectric $B_1$ phase, whereas 12OSOR, and 14OSOR exhibit antiferroelectric $B_2$ phase.

All these materials have been also studied by texture observations and reversal current method. For $B_2$ phases of 12OSOR and for 14OSOR quasi-planar and quasi-homeotropic textures were observed. Polarization for $B_1$ phase of 9OSOR is rather small and it increases with temperature. For $B_2$ phases of 12OSOR, and 14OSOR the spontaneous polarization is very high (about $600\,nC/cm^2$). Shorter homologue 8OSOR has been investigated by us and it shows $B_1$ phase which displays some ferroelectric properties [8]. Bent-core compounds with different configurations of thioester's group have been studied in [9].

## 2. Experimental

### 2.1. *Synthesis*

The synthesis of banana-shaped homologoues 1,3-phenylene bis{4-[(4-alkoxybenzoyl) sulfanyl]benzoate}, referred to as nOSOR, where n denotes the number of carbon atoms in the terminal alkoxy chain, is outlined schematically in Figure 2. These compounds have ester and thioester connecting groups and are derived from resorcinol as the central core. These banana-shaped molecules correspond to the formula shown in Figure 1.

The 4-[(4′-alkoxybenzoyl)sulfanyl]benzoic acids (nOSB, IV) were obtained by reaction of chlorides (II), of the appropriate 4-n-alkoxybenzoic acids (nOB, I) with 4-mercaptobenzoic acid (III). This process was carried out at room temperature, in the presence of pyridine in toluene. Crude acids (nOSB) were purified by repetitive crystallization from ethyl acetate until constant melting points were achieved.

The final products (VII) were synthesized by two methods: first the acids nOSB (IV) were esterified with resorcinol in the presence of 1,3-dicyclohexylcarbodiimide (DCC) and dimethylaminopyridine (DMAP) in dichloromethane (as solvent) at the room temperature and second along the path a traditional synthetic route by reaction of 4-(4′-n-alkoxybenzoylthio)benzoic acid chloride (V) and resorcinol (VI) in toluene in the presence of pyridine at 40–50°C (Fig. 1). The progress of the reaction was monitored by thin layer chromatography (TLC). The first method is much quicker, however its yield is quite poor (24%). This is why the second method, of 47% yield, is preferred.

All the final liquid crystal compounds were purified by means of column chromatography with silica gel filling (Merck, 60, 0.063 – 0.2 mm) and methyl dichloride

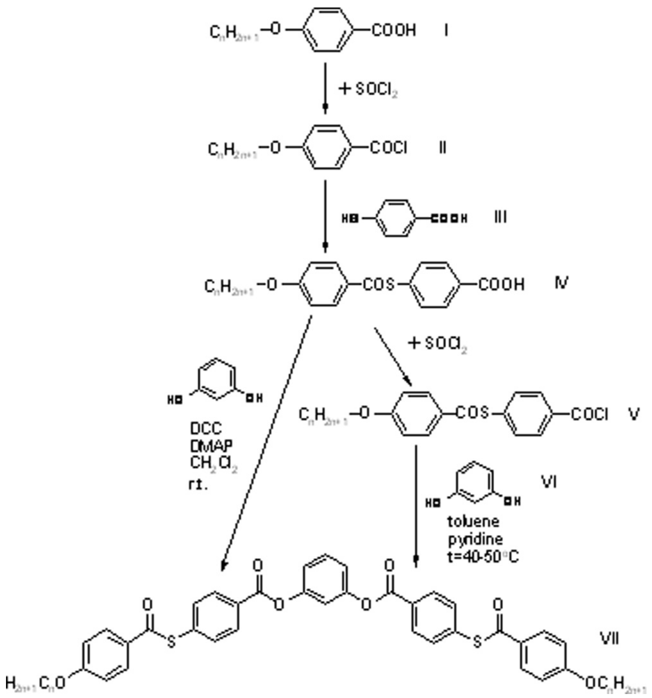

Figure 2. General synthetic pathway used for the preparation of banana-shaped nOSOR mesogens.

as eluent. Crude nOSORs were crystallized from mixture: ethyl alcohol and acetate–ethyl until constant melting points were achieved. At last, their structure was confirmed by spectroscopic methods: $^{1}$H NMR,$^{13}$C NMR, MS and FT-IR.

## 2.2. *Experimental Methods*

Electrooptic measurements and texture observations were done using Nikon Eclipse Polarizing Microscope LV100POL and INSTEC temperature controller. Texture observations and studies of electro-optic switching between the planar and homeotropic textures for 12OSOR were done at LEMCEL using Olympus Polarizing Microscope BX60 and LINKAM temperature controller. To observe textures in electro-optic cell under high fields a wave form generator Agilent 33120A and F20A amplifier were employed.

Texture observations allowed us to identify phases. 9OSOR compound shows ferroelectric $B_1$ phase, however, 12OSOR, and 14OSOR show antiferroelectric $B_2$ phase. Using thin AWAT cells with ITO electrodes it was possible to observe electro-optic switching between quasi-planar and quasi-homeotropic textures for $B_2$ phase of 12OSOR compounds. In Figure 3 one can see a transition between these two states.

In Figure 3(a) one can see a characteristic texture of extinction crosses observed under triangular electric field. A transition from quasi-planar (bright state, Figure 3(a)), in which bent-core molecules "are parallel" to electrode's surface and their smectic planes are rolled up in onion-like circular cylinders [5,6], to the dark

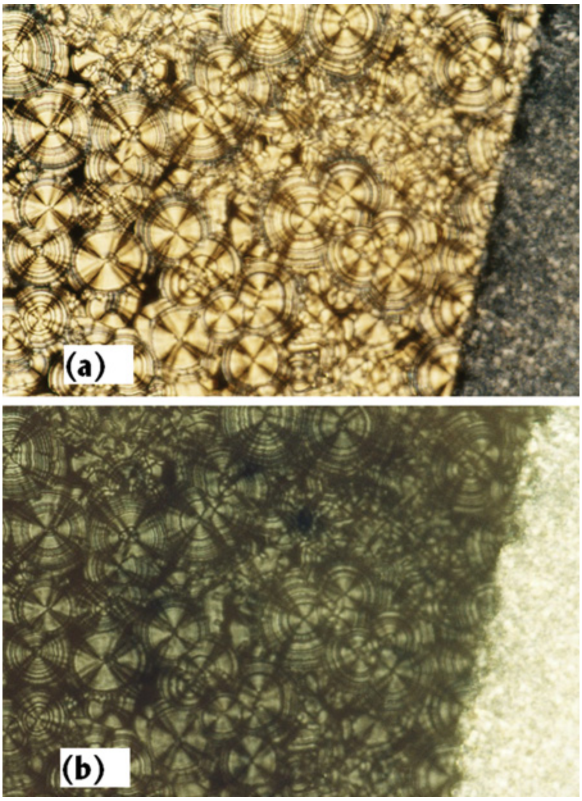

**Figure 3.** Switching between planar and homeotropic texture of 12OSOR's $B_2$ phase, (a) Quasi-planar texture of the $B_2$ phase in thin 1.7 μm AWAT cell (T = 112°C), (b) Quasi-homeotropic texture of $B_2$ phase under electric field of 13 $V_{p\text{-}p}/\mu m$ (T = 112°C). (Figure appears in color online.)

state (quasi-homeotropic, Figure 3(b)). One should add that at a certain voltages of triangular wave a completely dark state shows up in which the secondary optical axis is normal to the electrodes. The character of the texture changes under triangular electric field suggests that 12OSOR exhibits an anticlinic, antiferroelectric phase ($SmC_aP_A$).

The measurements of spontaneous polarization were done by reversal current method using Agilent 33120A wave form generator and F20A amplifier. Both the driving voltage and the response current spectra of the samples were recorded on the Agilent DSO6102A digital scope and transferred by LAN connection to the computer. Temperature of the sample was controlled by means of INSTEC hot stage driven by the computer.

Dielectric studies have been performed by using a dielectric spectrometer based on Agilent 4294A impedance analyzer controlled by PC. The sample was put into the capacitor consisting of two glass plates covered with gold layers separated by 5 μm spacers (AWAT HG cells). The cell was calibrated by using standard liquids. The substances being in isotropic phase were introduced into cells by means of capillary effect.

## 3. Results and Discussion

Spontaneous polarization measurements confirmed, that the $B_1$ phase of 9OSOR is a ferroelectric one – a single peak was observed (Fig. 4(a)) – and $B_2$ phase of 12OSOR, and 14OSOR exhibits antiferroelectric phase – two well separated peaks were detected as a response current (Fig. 4(b)). Polarization for phase $B_1$ of 9OSOR is rather small and it's temperature dependence is unusual for ferroelectric liquid crystals – it increases with temperature (Fig. 5(a)). For $B_2$ phase of 14OSOR spontaneous polarization is very high (Fig. 5(b)) – it is close to 600 nC/cm$^2$ and slightly smaller than for 12OSOR [4].

Dielectric measurements were done using dielectric spectrometer based on Agilent 4294A impedance analyzer. The dielectric spectra measured for $B_1$ phase of 9OSOR without and with bias voltage show only one Debye-type dielectric relaxation process (Fig. 6(a)) connected with molecule reorientation around the short axis. For $B_2$ phase of 12OSOR, and 14OSOR dielectric spectra measured with bias voltage show two well separated relaxation processes (Fig. 6(b)).

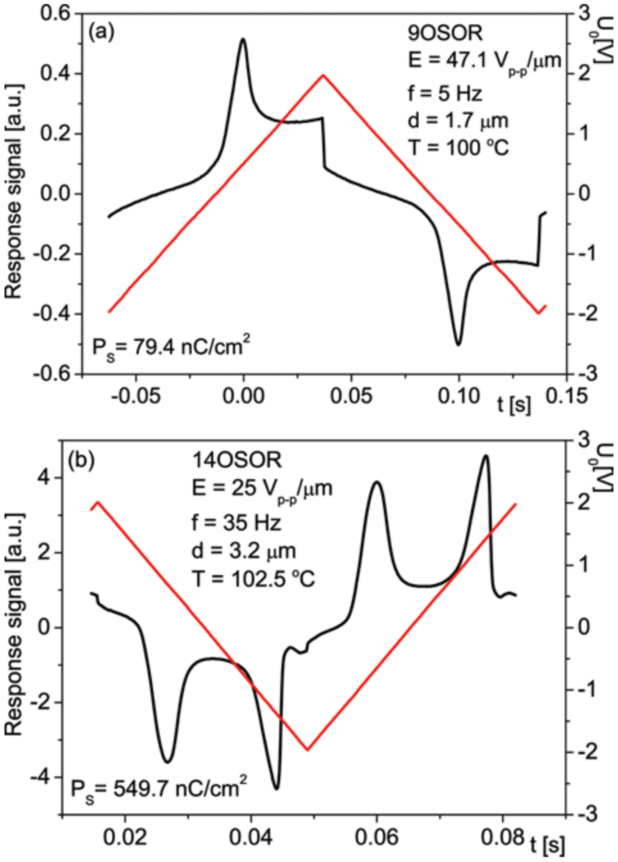

**Figure 4.** Reversal current spectra obtained for $B_1$ (a) and $B_2$ (b) phases. (Figure appears in color online.)

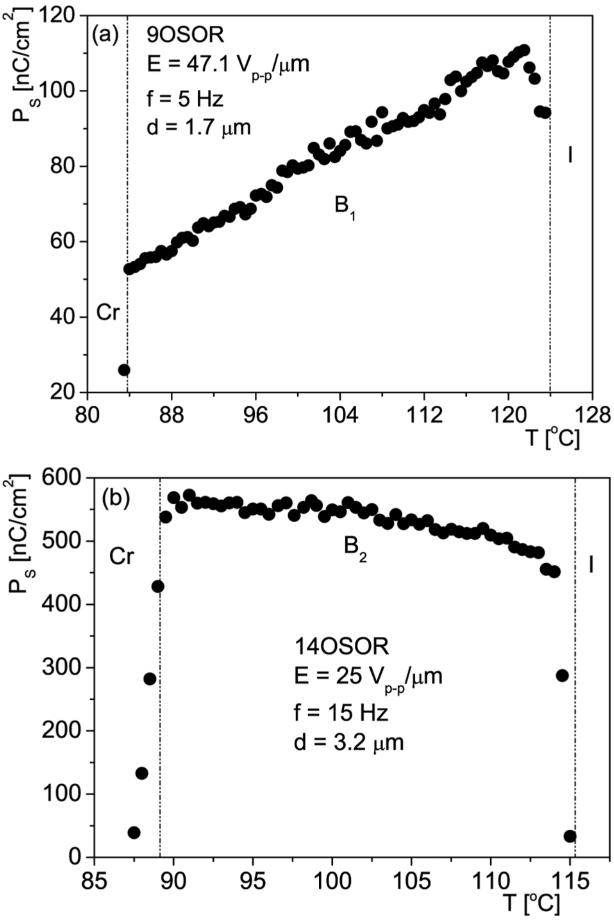

**Figure 5.** Spontaneous polarization vs. temperature obtained for (a) ferroelectric $B_1$ phase of 9OSOR – $E = 42.4\,V_{p\text{-}p}/\mu m$, $f = 5\,Hz$, $d = 1.7\,\mu m$ and for (b) antiferroelectric $B_2$ phase of 14OSOR compound – $E = 25\,V_{p\text{-}p}/\mu m$, $f = 15\,Hz$, $d = 3.2\,\mu m$.

The following complex function [10,11] was fit to the experimental points measured without bias field:

$$\varepsilon^*(\nu) = \varepsilon(\infty) + \frac{\varepsilon(0) - \varepsilon(\infty)}{1 + (i2\pi\nu\tau)^{1-\alpha}} - \frac{iA}{\varepsilon_0 \nu M} + \frac{B}{\nu^N}, \tag{1}$$

where $\varepsilon(\infty)$ is a high frequency electric permittivity, $\varepsilon_0$ – electric permittivity of the free space, $\varepsilon(0)$ – static electric permittivity, $\tau$ – relaxation time, $\alpha$ – distribution parameter of relaxation times ($0 \le \alpha \le 1$), $\sigma(\nu)$ – ionic conductivity, $\nu$ is a frequency and $A, B, M, N$ – phenomenological fitting parameters, where $A = \frac{\sigma(\nu)}{(2\pi)^M}$. Solid lines in Figure 6(a) and (b) are theoretical fit curves of Eq. (1) to the experimental points.

To the experimental points obtained under the bias field (Figure 6(b)) the following complex fitting function was used:

$$\varepsilon^*(\nu) = \varepsilon(\infty) + \frac{\varepsilon_1(0) - \varepsilon(\infty)}{1 + (i2\pi\nu\tau_2)^{1-\alpha_2}} - \frac{\varepsilon_1(0) - \varepsilon_1(0)}{1 + (i2\pi\nu\tau_1)^{1-\alpha_1}}, \tag{2}$$

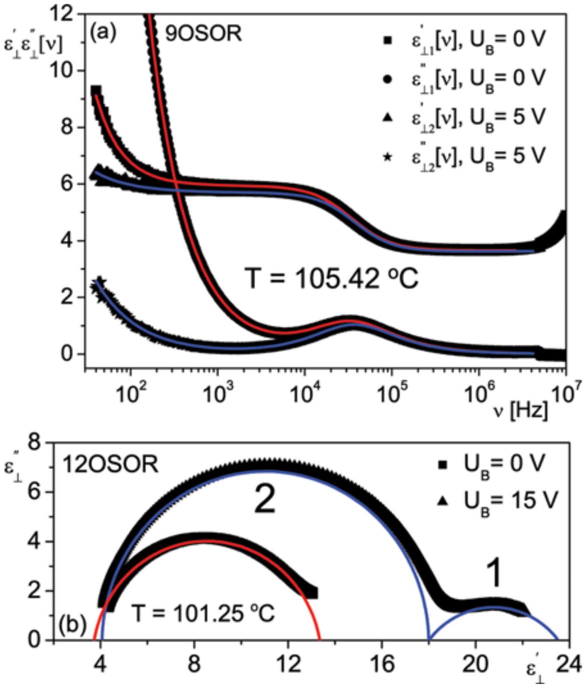

**Figure 6.** Dispersion and absorption curves for 9OSOR (a) and Cole-Cole plot (b) of the dielectric spectra acquired for 12OSOR.

where $\varepsilon(\infty)$ is a high frequency electric permittivity, $\varepsilon_0$ – electric permittivity of the free space, $\varepsilon(0)$ – static electric permittivity, $\varepsilon_1(0)$ – quasi-static electric permittivity, $\tau_1$ and $\tau_2$ – are relaxation times, $\alpha_1$ and $\alpha_2$ – distribution parameters of relaxation times $(0 \le \alpha_i \le 1)$ and $\nu$ is a frequency.

The dielectric spectra were measured in the frequency range from 40 Hz to 10 MHz. The dielectric spectra acquired incorporate about 80 points pear decade.

In low frequency range the relaxation process is connected with fluctuations of domains. In high frequency range – it is connected with reorientation around the long axis and it is also observed without bias field. The value of activation energy obtained for this process (Fig. 7(b)) substantiates such interpretation. For 12OSOR the dielectric relaxation process observed without bias field is at low frequencies influenced by ionic conductivity. The fitting parameters are gathered in Table 1.

The low frequency range the relaxation process (**1**) is connected with fluctuations of ferroelectric domains. It is a low frequency process which is merged with conductivity contribution in the absence of the bias field. After application of the bias field process (**1**) is clearly seen (Fig. 6(b)). However, it displays a large value (0.42) of the distribution parameter (Table 1) which makes the Cole-Cole plot far from being a semi-circle. Similar results have been obtained for 14OSOR (Table 2).

It was found that all materials studied exhibit unusual frequency dependence of $\varepsilon'(\nu)$ and $\varepsilon''(\nu)$ at low frequencies. Dielectric measurements show also that at low frequencies there is an electrode polarization contribution to the dielectric permittivity and the electrical ionic conductivity contribution to the dielectric loss for all materials studied. However, the electric conductivity of these banana-shaped thioesters is

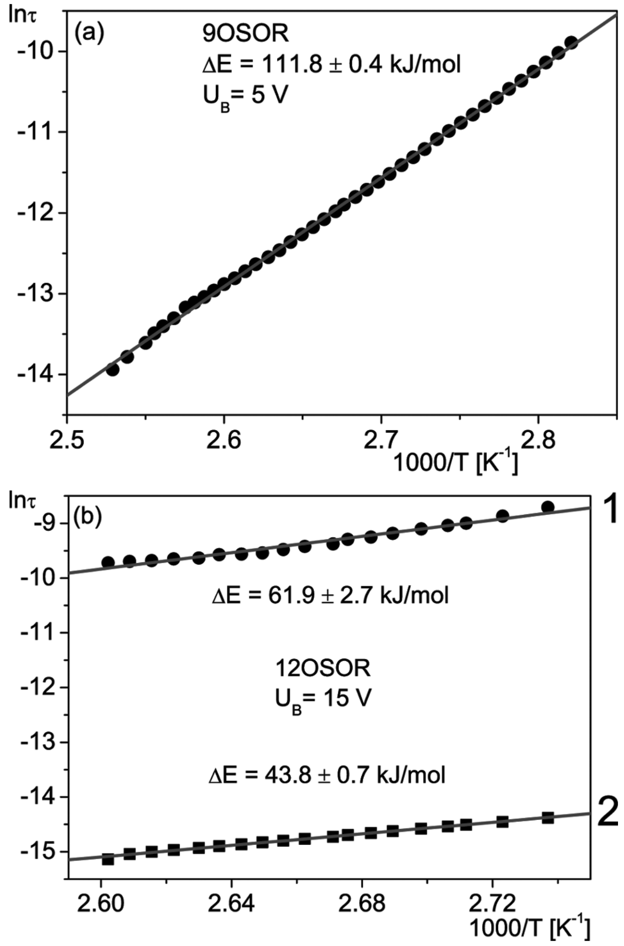

**Figure 7.** (a) Arrhenius plot for the dielectric relaxation process for 9OSOR $B_1$ phase observed with bias voltage equal to 5 V, (b) Arrhenius plots for the dielectric relaxation processes for 12OSOR $B_2$ phase observed with bias voltage equal to 15 V.

distinctly lower than for other bent-core compounds studied before [12]. The M parameter for all materials studied shows the difference between calamitic LCs and B phases. One should notice that under bias field M = 1 for $B_2$ phases of both

**Table 1.** Fitting parameters for three relaxation processes shown in Figure 6(b) for $B_2$ phase of 12OSOR

| 12OSOR | T = 101.25°C | | | | | | |
|---|---|---|---|---|---|---|---|
| $U_B$ [V] | Proces | ε (0) | τ [s] | α | ε (∞) | σ [S/m] | M |
| $U_B = 15$ | —1 | 23.5 | 1 · E-4 | 0.42 | 18 | 0 | 1 |
| | —2 | 18 | 4 · E-7 | 0.01 | 4.1 | 6 · E-11 | 1 |
| $U_B = 0$ | — | 13.4 | 4 · E-7 | 0.12 | 3.7 | 3.9 · E-9 | 0.6 |

**Table 2.** Fitting parameters for three relaxation processes for $B_2$ phase of 14OSOR

| 14OSOR | T = 100°C | | | | | | |
|---|---|---|---|---|---|---|---|
| $U_B$ [V] | Proces | ε (0) | τ [s] | α | ε (∞) | σ [S/m] | M |
| $U_B = 10$ | —1 | 29.3 | 1.3 · E-4 | 0.48 | 19.4 | 0 | 1 |
| | —2 | 19.4 | 6 · E-7 | 0.06 | 3.9 | 3 · E-8 | 1 |
| $U_B = 0$ | — | 15.7 | 5.9 · E-7 | 0.07 | 3.9 | 3.8 · E-9 | 0.6 |

12OSOR (Table 1) and 14OSOR (Table 2) as it has been found for nematic and orthogonal smectic phases [13] without applying any bias field.

## 4. Conclusions

The dielectric spectra measured for $B_1$ phase of 9OSOR with and without bias voltage showed only one dielectric relaxation process connected with molecular reorientation around the short axis. However, for $B_2$ phase of 12OSOR, and 14OSOR the dielectric spectra measured with bias voltage show two well separated relaxation processes. In low frequency range the relaxation process is connected with fluctuations of domains. In high frequency range – it is connected with reorientation around the long axis and it is also observed without bias field. For 12OSOR the dielectric relaxation process observed without bias field is complex: in the high temperature range of $B_2$ phase it is connected with molecular reorientation around the short molecular axis, whereas in the low temperature range – around the long axis.

Dielectric measurements showed also that at low frequencies there is an electrode polarization contribution to the dielectric permittivity and the electrical ionic conductivity contribution to the dielectric loss for all materials studied. The electric conductivity of these banana-shaped thioesters is distinctly lower than for other similar compounds. The M parameter for all materials studied shows the difference between calamitic LCs and B phases.

## Acknowledgment

Financial support of Polish Ministry of Science and Higher Education in scope of Grant NN202 076435 is gratefully acknowledged.

The research was carried out with the equipment purchased thanks to the financial support of the European Regional Development Fund in the framework of the Polish Innovation Economy Operational Program (contract no. POIG.02.01. 00-12-023/08).

## References

[1] Noiri, T., Sekine, T., Watanabe, J., Furukawa, T., & Takezoe, H. (1996). *J. Mater. Chem.*, *6*, 1231.

[2] Sekine, T., Takanishi, Y., Noiri, T., Watanabe, J., & Takezoe, H. (1997). *Jpn. J. Appl. Phys.*, *36*, L1201.

[3] Ossowska-Chruściel, D., Kudłacz, K., Sikorska, A., Chruściel, J., Marzec, M., Mikułko, A., Wróbel, S., Douali, R., & Legrand, Ch. (2007). *Phase Transit.*, *80*, 781.

[4] Wierzejska-Adamowicz, M., Ossowska-Chruściel, D. M., Czerwiec, J., Douali, R., Legrand, Ch., Chruściel, J., Marzec, M., & Wróbel, S. (2010). *Optical Rev.*, *17*(4), 1–6.

[5] Reddy, R. A., & Tschierske, C. (2006). *J. Mater. Chem.*, *16*, 907.

[6] Vaupotič, N. (2006). *Ferroelectrics*, *344*, 151.

[7] Kue Lee, S., Kang, S., Tokita, M., & Watanabe, J. (2010). *Liq. Cryst.*, *37*(5), 593–598.

[8] Ossowska-Chruściel, D., Kudłacz, K., Sikorska, A., Chruściel, J., Marzec, M., Mikułko, A., Wróbel, S., Douali, R., & Legrand, Ch. (2007). *Phase Transit.*, *80*, 781.

[9] Rouillon, J., Marcerou, J., Laguerre, M., Nguyen, H., & Achard, M. (2001). *J. Mater. Chem.*, *11*, 2946.

[10] Vakhovskaya, Z., Weissflog, W., Friedemann, R., & Kresse, H. (2007). *Phase Transit.*, *80*, 705.

[11] Kresse, H. (2003). Dielectric behavior of phases formed by bent-shaped molecules. In: *Relaxation Phenomena*, Haase, W. & Wróbel, S. (Eds.), Springer-Verlag: Berlin Heidelberg, Section 5.7, pp. 400–421.

[12] Wróbel, S., Haase, W., Kilian, D., Chien, L.-C., & Chong-Kwang, L. (2000). *Ferroelectrics*, *243*, 277.

[13] Mikułko, A., Fraś, M., Marzec, M., Wróbel, S., Ossowska-Chruściel, M. D., & Chruściel, J. (2008). *Acta Phys. Polonica*, *113*, 1155.